

Received: 2016.12.05  
Accepted: 2017.01.02  
Published: 2017.01.14

# Jolkinolide A and Jolkinolide B Inhibit Proliferation of A549 Cells and Activity of Human Umbilical Vein Endothelial Cells

Authors' Contribution:  
Study Design A  
Data Collection B  
Statistical Analysis C  
Data Interpretation D  
Manuscript Preparation E  
Literature Search F  
Funds Collection G

ABE 1,2 **Lei Shen**  
CF 2 **Shan-Qiang Zhang**  
B 1 **Lei Liu**  
BD 1 **Yu Sun**  
CF 2 **Yu-Xuan Wu**  
DE 2 **Li-Ping Xie**  
AG 1 **Ji-Cheng Liu**

1 Qiqihar Institute of Medical and Pharmaceutical Sciences, Qiqihar Medical University, Qiqihar, Heilongjiang, P.R. China  
2 Department of Anatomy, Qiqihar Medical University, Qiqihar, Heilongjiang, P.R. China

**Corresponding Author:** Jicheng Liu, e-mail: [qyliujc@yahoo.com](mailto:qyliujc@yahoo.com)

**Source of support:** This work was supported by the National Science Foundation of China (81573660)

**Background:** Jolkinolide A (JA) and Jolkinolide B (JB) are diterpenoids extracted from the roots of *Euphorbia fischeriana* Steud and have been shown to have anti-tumor activity. However, their effects on the ability of tumor cells to invade blood vessels and metastasize remain largely unknown. Investigations into the effects of JA and JB on the angiogenesis of tumor tissues may facilitate the identification of new natural drugs with anti-tumor growth and metastasis activities.

**Material/Methods:** We used different concentrations of JA and JB (20 µg/ml, 40 µg/ml, 60 µg/ml, 80 µg/ml, and 100 µg/ml) to stimulate A549 cells and then studied the effects on the growth and metastasis of lung cancers. In addition, we used conditional media from A549 cells (A549-CM) stimulated by either JA or JB in different concentrations to culture human umbilical vein endothelial cells (HUVECs).

**Results:** We found that both JA and JB significantly inhibited the Akt-STAT3-mTOR signaling pathway and reduced the expression of VEGF in A549 cells, but JB exhibited more significant inhibitory effects than JA. The JB-stimulated A549 cell conditional media had a greater inhibitory effect on the proliferation and migration of HUVECs than did the conditional media of JA-stimulated A549 cells. This effect gradually increased with increasing concentrations of either type of Jolkinolide.

**Conclusions:** Our results suggest that JA and JB inhibited VEGF expression in A549 cells through the inhibition of the Akt-STAT3-mTOR signaling pathway, and directly inhibited the proliferation and migration of HUVECs. These findings are of great significance for the development of new plant-derived chemotherapy agents for the treatment of cancer.

**MeSH Keywords:** **Angiogenesis Inhibitors • Cell Movement • Cell Proliferation • Diterpenes • Herbal Medicine • Human Umbilical Vein Endothelial Cells**

**Full-text PDF:** <http://www.medscimonit.com/abstract/index/idArt/902704>



## Background

The deadliest forms of cancer are breast, colon, and prostate cancers, which result in approximately half of the cancer deaths in both men and women worldwide [1–3]. Distinct treatment strategies, such as surgery, chemotherapy, and radiation therapy, have been widely applied in clinical practice to inhibit tumor growth and prevent the metastasis of tumor cells via blood vessels. While these strategies are effective for cancer treatment, their intrinsic adverse effects cause major problems, such as the inhibition of hematopoietic function and immunity that accompanies chemotherapy [4]. Therefore, treatment strategies that successfully inhibit tumor growth and angiogenesis with limited adverse effects are highly sought in cancer research.

Tumorigenesis and development are complicated processes, in which numerous molecules and pathways are involved. A number of studies have focused on natural anti-tumor drugs that have shown significant tumor growth inhibition with few adverse effects [6,7]. *Euphorbia fischeriana* is a perennial herbaceous plant of the *Euphorbia* genus and has long been used to treat breast, lung, gastric, and other malignant tumors in China and South Korea, as well as other Asian countries [8,9]. These studies have found that *E. fischeriana* and other plants from the *Euphorbia* genus were effective in treating pleural effusion and ascites by reducing tissue swelling and exudation, among other inflammatory responses [10,11]. In addition, it has been reported that *E. fischeriana* Steud is able to reduce the inflammatory responses of macrophages induced by lipopolysaccharides in mice [10,12,13]. Moreover, *Synadenium umbellatum* Pax (SU) and other plants of the *Euphorbia* genus have also been demonstrated to have anti-angiogenic effects [14]. Nevertheless, the acting mechanisms of *E. fischeriana* Steud are not clearly understood.

Approximately 60 types of compounds, such as diterpenoids, triterpenoids, flavonoids, and volatile oils, have been identified in *E. fischeriana* roots [15]. Of these, the diterpenoids include JA, JB, 12-Deoxyphorbol 13-palmitate, and many other monomers [15]. A number of studies have shown that 12-Deoxyphorbol 13-palmitate, JB, and other monomers significantly inhibit the proliferation of gastric tumor and breast cancer cells [16–18]. 12-Deoxyphorbol 13-palmitate has been proven to inhibit the expression of VEGF and HIF-1 $\alpha$  in MCF-7 cells through the Akt signaling pathway, which subsequently reduced the activity of human umbilical vein endothelial cells (HUVECs) [19,20]. However, the inhibitory mechanisms of JA and JB on the proliferation and migration of HUVECs in lung cancer are not fully understood.

In light of these results, we hypothesize that JA and JB have potential inhibitory effects on HUVEC proliferation. In the present

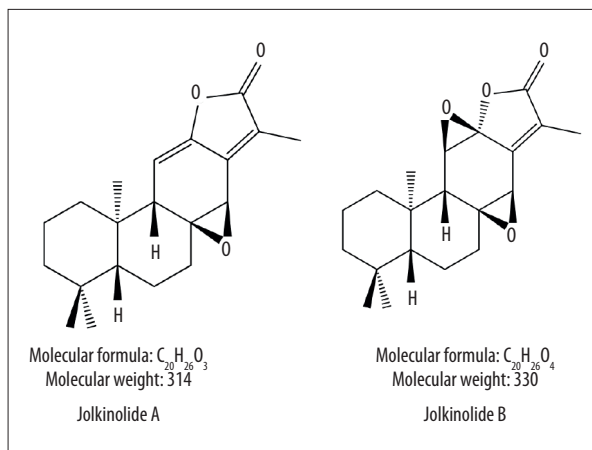


**Figure 1.** Chemical structures of Jolkinolide A (JA) and Jolkinolide B (JB).

study, different concentrations of JA and JB were separately used to stimulate A549 cells to obtain A549 conditional media, which was then used to stimulate HUVECs. Our results demonstrate that JA and JB reduced the expression of VEGF in A549 cells through the inhibition of the Akt-STAT3-mTOR signaling pathway, and inhibited HUVEC proliferation and migration. This suggests that JA and JB inhibit tumor angiogenesis.

## Material and Methods

### JA and JB extraction

JA and JB were extracted from dry *E. fischeriana* Steud roots (Qiqihar Medical Science Research Institute, Qiqihar, China) according to the methods used in a previous study [21]. Their determined purity exceeded 99% (Figure 1). The extracted JA and JB were dissolved in dimethyl sulfoxide (DMSO, Sigma, St. Louis, MO, USA) and were mixed in a series of concentrations (20  $\mu$ g/ml, 40  $\mu$ g/ml, 60  $\mu$ g/ml, 80  $\mu$ g/ml, and 100  $\mu$ g/ml) for use in the subsequent experiments. The final concentration of DMSO in the culture medium for *in vitro* experiments was <0.01%.

### A549 cell culture and experimental groups

The A549 human lung cancer cells were purchased from American Type Culture Collection (ATCC, Rockville, MD, USA). A medium containing RPMI-1640 (Gibco, Grand Island, NY, USA), penicillin (100 U/ml), streptomycin (100 mg/ml) (Shanghai Sangon Biotech. Co., Shanghai, China), and 10% fetal bovine serum (Gibco, Gaithersburg, MD, USA) was used as the basic A549 medium. A549 cells of passages 3 and 5 were used in both the *in vivo* and *in vitro* experiments. The cultures showed no evidence of crisis or senescence during the of the experiments. JA and JB of different concentrations (20  $\mu$ g/ml, 40  $\mu$ g/ml

ml, 60 µg/ml, 80 µg/ml, and 100 µg/ml) were used to stimulate the A549 cells, which were grouped into JA-A549 and JB-A549 groups according to the concentration. Neither JA nor JB were added to the control group.

RPMI-1640, which contained 20 µg/ml, 40 µg/ml, 60 µg/ml, 80 µg/ml, or 100 µg/ml of JA or JB and 1% FBS, was used to culture the A549 cells ( $2 \times 10^6$ ) at 37°C and 5% CO<sub>2</sub> for 24 h. According to the different concentrations, the supernatants of the JA-A549 and JB-A549 groups were collected by centrifugation at 1000 rpm/min for 5 min. The supernatants were then filtered with a 0.22-µm filter (Corning, NY, USA) and stored at -80°C until use.

### HUVEC culture and experimental groups

HUVECs were obtained from the Procell Company (Procell Ltd., Wu Han, China) and the basic HUVEC medium consisted of Ham's F12K medium (Gibco, NY, USA), 100 U/ml penicillin, 100 mg/ml streptomycin (Shanghai Sangon Biotech. Co., Shanghai, China), and 10% fetal bovine serum (FBS; Gibco, Gaithersburg, USA). HUVECs between passages 4 and 6 were used for both *in vivo* and *in vitro* experiments. During these experiments, none of the cultures showed evidence of crisis or senescence. The supernatants of varying concentrations from the JA-A549 and JB-A549 groups were diluted with Ham's F12K medium with 1% FBS [conditioned medium (CM)] at a 1: 5 ratio. These conditioned media are referred to as JA-A549-CM and JB-A549-CM. The HUVEC experimental grouping was determined by the corresponding concentration of conditioned medium. In addition, JA and JB of different concentrations (20 µg/ml, 40 µg/ml, 60 µg/ml, 80 µg/ml, and 100 µg/ml) were used to stimulate the HUVECs, which were grouped into JA-HUVEC and JB-HUVEC groups according to the concentration. Normal cultured HUVECs were used as the non-conditioned medium (NCM group), or control group.

### Liquid chromatography

The supernatants of each group were collected, and the Jolkinolide residues were detected using an e2695 HPLC-2489 UV/Vis Detector (Waters, Milford, MA, USA). The liquid chromatography conditions were set as follow. The SunFire™ C18 chromatographic column parameters were set to 250×4.6 mm and 5 µm (Waters, Milford, MA, USA) and 70% methyl alcohol (Merck KGaA, Darmstadt, Germany) and 30% H<sub>2</sub>O were used in the mobile phase. The temperature of the chromatographic column was set to 35°C, the volume of sample injection was 10 µL, and the detection wavelength was  $\lambda=254$  nm [9].

### MTT assay

A 3-(4, 5-dimethylthiazol-yl)-2, 5-diphenyltetrazoliumbromide (MTT) assay was used to detect A549 and HUVEC proliferation.

Both cell types were cultured in 96-well plates (Corning, USA) at  $8 \times 10^4$  cells/well. JA and JB at 20 µg/ml, 40 µg/ml, 60 µg/ml, 80 µg/ml, and 100 µg/ml concentrations were added into separate A549 cells or HUVECs. In addition, the conditioned medium from each group was added into another  $8 \times 10^4$  cells/well with HUVECs. The cells were incubated at 37°C and 5% CO<sub>2</sub> for 24 h and the MTT assay was performed by adding 5 mg/ml MTT (Sigma, USA) to each well for 4 h at 37°C. The supernatant from each well was then removed, 100 µl dimethyl sulfoxide (DMSO, Sigma) was added, and the samples were shaken for 10 min, whereupon the absorbance value (OD) of each well was measured using an Emax microplate reader (Molecular Devices, Sunnyvale, CA, USA) at 490 nm.

### Annexin V-FITC staining experiments

The HUVECs were cultured in 24-well plates (Corning, USA) at  $3 \times 10^5$  cells/well. According to the HUVEC groupings, the cells from each group were incubated at 37°C and 5% CO<sub>2</sub> for 24 h and the original medium was discarded, whereupon pre-cooled 0.01 mmol/L phosphate- buffered saline (PBS, Boster Ltd., Wuhan, China) was added. The cells were centrifuged at 1000 rpm/min for 10 min, 3 times each, before being re-suspended with 200 µL Binding Buffer (Boster Ltd., Wuhan, China). Next, 20 µg/ml Annexin V-FITC (Biolegend, San Diego, CA, USA) was added, and the cells were incubated in the dark for 30 min at 4°C. The cells that had been labeled with Annexin V-FITC were observed with a BX53 fluorescence microscope (Olympus Optical Co., Ltd, Japan), and the cell apoptosis numbers were calculated using Image-Pro Plus 7.0 image analysis software (Mediacy Cybernetics, Inc. Bethesda, MD, USA).

### Cell scratch experiments

HUVECs were seeded at  $2 \times 10^6$  cells/well in 6-well plates (Corning, USA). A central scratch was created by scraping cells away with the tip of a p1000 pipette (Axygen, Tewksbury, MA, USA) and the HUVECs were then washed 3 times with 0.01 mmol/L PBS. According to the HUVEC groupings, cells were cultured with the appropriate conditioned medium or different concentrations of JA or JB, as well as 2 mmol/L hydroxyurea (Sigma, USA). They were then incubated at 37°C in 5% CO<sub>2</sub> for 24 h. The cells were fixed with 4% paraformaldehyde (Amquar Ltd., Shanghai, China) for 6 h after being washed again 3 times with 0.01 mmol/L PBS, and the HUVEC scratches were stained with 1% crystal violet (Amquar Ltd., China). The scratches were recorded with a BX53 microscope (Olympus, Japan), and the cell scratch areas at 0 and 24 h were measured using Image-Pro Plus 7.0 software (Media Cybernetics, USA). The closure rate of the cell scratch areas at 24 h was calculated as (cell scratch area at 0 h – cell scratch area at 24 h/cell scratch area at 0 h) ×100%.

### Transwell chamber experiments

HUVECs were resuspended in Ham's F12K medium with 1% FBS, and were placed in the upper chamber of 25 mm, 8.0  $\mu\text{m}$  transwell cell chambers (Corning, USA) at  $1 \times 10^4$  cells/well. The conditioned medium from each group at different concentrations of JA or JB was added to the lower chambers. The cells were incubated at 37°C in 5%  $\text{CO}_2$  for 12 h and the residual cells in the transwell chambers were removed and washed 3 times with 0.01 mmol/L PBS. The cells that migrated to the other side of the membrane were fixed with 4% paraformaldehyde (Amquar China Ltd., China) for 6 h and stained with 1% crystal violet (Amquar China Ltd., China), photos were taken using a BX53 microscope (Olympus, Japan), and the cell migration rate at 12 h was measured using Image-Pro Plus 7.0 software (Media Cybernetics, USA) and was calculated as (migrated cells at 12 h/ $1 \times 10^4$ )  $\times 100\%$  [22].

### Western blot experiments

In total,  $5 \times 10^6$  A549 cells and HUVECs were each cultured. The conditioned medium of each group at different concentrations of JA and JB was added into the cells, which were then incubated at 37°C in 5%  $\text{CO}_2$  for 24 h, before being lysed and centrifuged at 12 000 rpm at 4°C for 10 min. The protein concentrations were measured with a BCA kit (Beyotime Biotechnology, Shanghai, China). A 25- $\mu\text{g}$  sample of each group was extracted, and SDS-PAGE gel electrophoresis (BIO-RAD Laboratories, Hercules, CA, USA) was performed at 100 V for 90 min. A sample from each group was then transferred to polyvinylidene fluoride membranes (PVDF, Millipore, Billerica, MA, USA) with an aperture of 0.2  $\mu\text{m}$ . Next, mouse anti-human caspase 9 primary antibody (1: 200, Santa Cruz, CA, USA), mouse anti-human Akt primary antibody (1: 700, Santa Cruz, CA, USA), mouse anti-human STAT3 primary antibody (1: 700, Abcam, Cambridge, UK), and mouse anti-human mTOR primary antibody (1: 550, Santa Cruz, USA) were all added. After incubation overnight at 4°C, a horseradish-peroxidase (HRP)-linked secondary antibody and a conjugated goat anti-mouse IgG antibody (1: 200, Abcam, UK) were added, and the membrane was continuously incubated at room temperature for 90 min. The protein expression levels were measured using enhanced chemiluminescence (ECL, GE Healthcare, UK), and the relative absorbance value of each protein band was measured using Image-Pro Plus 7.0 software.  $\beta$ -actin (Abcam, Cambridge, UK) was used as an internal control.

### Enzyme-linked immunosorbent assay (ELISA)

The supernatant from each A549 cell group was collected and a quantitative enzyme-linked immunosorbent assay kit (R&D Systems, Minneapolis, MN, USA) was used to analyze the A549 supernatant from each group, according to the manufacturer's

instructions. The supernatant of normal cultured A549 cells was used as the negative control.

### Animal experiments

All animal procedures were approved by the Qiqihar Medical University Committee on Animal Experimentation, and complied with the NIH guidelines for the care and use of laboratory animals. We used 4–5-week-old female BALB/c nude mice (Qiqihar Institute of Medical and Pharmaceutical Sciences, Qiqihar, China) in all of the experiments. Approximately  $6 \times 10^5$  A549 cells were resuspended with 100  $\mu\text{l}$  of 0.01 mmol/L PBS and were subcutaneously inoculated into the right and left flanks ( $n=20$  in each group), and all mice were fed for 1 month. The mice were then divided into the PBS, JA, and JB groups. Next, 40 mg/kg of JA or JB and 0.01 mmol/L PBS were intraperitoneally administered once every 3 days for 2 months. All mice were fed for an additional 2 months. At the end of the experiment, the tumor tissues of the 3 groups were harvested, fixed with 4% paraformaldehyde, and embedded in paraffin. The processed tumor tissues were then harvested for immunohistochemistry using anti-VEGF primary antibody (1: 300, Santa Cruz, USA), horseradish-peroxidase (HRP)-linked secondary antibody, conjugated IgG antibodies (Santa Cruz, USA), and 0.05% DBA (Santa Cruz, USA). The VEGF expression of the xenograft tumors was assessed for histological quantitative analysis with a BX53 microscope (Olympus, Japan).

### Statistical analyses

Each experiment was repeated 3 times for each group. SAS (version 9.2, SAS Institute Inc., Cary, NC, USA) was used to perform *t* tests or analysis of variance (ANOVA). The results are expressed as the mean  $\pm$  standard error of the mean (SEM), and  $P < 0.05$  was considered to be statistically significant.

## Results

### The effects of Jolkinolides on A549 cells

To explore the effects of JA and JB on A549 cells, we used different concentrations of each to stimulate A549 cells. An MTT assay showed that, compared with the OD values of A549 cells stimulated by JA at the same concentrations, the OD values of A549 cells stimulated by JB (20  $\mu\text{g}/\text{ml}$ , 40  $\mu\text{g}/\text{ml}$ , 60  $\mu\text{g}/\text{ml}$ , 80  $\mu\text{g}/\text{ml}$ , and 100  $\mu\text{g}/\text{ml}$ ) were lower by 17.7%, 46.8%, 37.6%, 33.3%, and 25.8%, respectively (Figure 2A). In addition, the OD values of A549 cell proliferation significantly decreased with increasing concentration of JB (Figure 2A). We also observed that the space between the cells gradually increased, cells were dispersed, cell debris appeared, and the overall number of cells gradually decreased (Figure 2B, 2C). With increasing

JA and JB concentrations, an increased expression of caspase 9 was also detected in A549 cells, and the expression of caspase 9 in the JB-A549 groups showed a significant increase ( $P < 0.01$ ) (Figure 2D–2F). These results suggest that JB exhibited more significant inhibitory effects on A549 cells than did JA.

### **JA and JB reduced the expression of Akt-STAT3-mTOR proteins in A549 cells**

To determine the effects of the 2 forms of Jolkinolide on A549 cell protein expression, we analyzed the vasoactive components in the conditioned medium for each group and found that, in the JB-A549-CM groups, the VEGF content was only 68.03%, 60.80%, 52.21%, 52.01%, and 40.43% that of the concentrations for each corresponding JA-A549-CM group (Figure 3A). We concluded that the lower levels of the VEGF protein in the supernatants of tumor cells might be due to the inhibition of the relevant cell signaling pathways. We also found that, with increasing concentrations of both Jolkinolide A and B, the expression levels of Akt, STAT3, and mTOR proteins in A549 cells gradually decreased (Figure 3B–3E).

### **The effects of conditioned media on HUVEC proliferation and apoptosis**

To determine the effects of JA and JB on HUVEC proliferation and apoptosis, we performed liquid chromatography and found that there was no residual JA or JB in the supernatants of A549 cells (Figure 4A). Moreover, the HUVECs were cultured together with the conditioned medium from A549 cells that had been stimulated by either JA or JB. The MTT assay demonstrated that, compared with the JA-A549-CM groups, the OD values of HUVEC proliferation in the JB-A549-CM groups were 41.70%, 33.72%, 26.79%, 19.62%, and 15.57% lower, respectively (Figure 4B). The Annexin V-FITC experiment found that, compared with the JA-A549-CM groups, the number of HUVECs labeled with Annexin V-FITC in the JB-A549-CM groups increased by 1.03, 1.46, 1.58, 2.12, and 2.45 times (Figure 4C–4E), respectively. Throughout the experiment, we found that the supernatants of the A549 cells stimulated by JA or JB were able to inhibit the proliferation of HUVECs, suggesting that both JA and JB play important roles in inhibiting HUVEC activity.

### **The effects of conditioned media on HUVEC migration**

For the determination of the effects of the Jolkinolides-stimulated A549 conditioned media on the movement of HUVECs, we performed an HUVEC scratch experiment. Compared with the JA-A549-CM groups, the HUVEC scratch closure rates in the JB-A549-CM groups were 34.06%, 39.95%, 48.57%, 59.43%, and 68.94% lower, respectively (Figure 5A–5C). Next, we performed a HUVEC migration experiment in a transwell chamber and found that, compared with the JA-A549-CM

groups, the HUVEC migration rates in the JB-A549-CM groups decreased by 27.55%, 34.12%, 43.97%, 53.08%, and 67.12%, respectively (Figure 5D–5F). These results suggest that the Jolkinolides-stimulated A549 cell supernatants encouraged the inhibition of HUVEC migration. Nevertheless, whether Jolkinolides have a direct inhibitory effect on the activity of HUVEC remains a subject for future research.

### **The effects of JA and JB on HUVEC proliferation and apoptosis**

We used the above-mentioned different concentrations of JA or JB to stimulate HUVECs. Compared with the JA-HUVEC groups, the OD values of HUVEC proliferation in JB-HUVEC groups were 30.45%, 34.51%, 23.84%, 51.36%, and 49.23% lower, respectively (Figure 6A). We also found that the number of HUVECs labeled with Annexin V-FITC in the JB-HUVEC groups were 1.84, 2.38, 2.49, 2.74, and 3.22 times higher than those in the JA-HUVEC groups, respectively (Figure 6B–6D). These results suggested that JA and JB are both capable of significantly inhibiting HUVEC proliferation, as well as promoting HUVEC apoptosis.

### **The effects of JA or JB on HUVEC migration**

To determine the effects of JA and JB on HUVEC movement, we performed an HUVEC scratch experiment. The closure rates of JB-HUVEC groups were 38.9%, 21.99%, 10.54%, 12.17%, and 1.21 times lower, respectively, than in the JA-HUVEC groups (Figure 7A, 7B). Next, we performed a HUVEC migration experiment in a transwell chamber and found that, compared with the JA-HUVEC groups, the HUVEC migration rates of the JB-HUVEC groups were lower by 6.52%, 10.39%, 15.86%, 30.13%, and 16.55%, respectively (Figure 7C, 7D). These results indicate that both JA and JB can directly inhibit the migratory activity of HUVECs.

### **Jolkinolides-induced reduction of Akt-STAT3-mTOR protein expression in HUVECs**

The protein expressions of each JA-HUVEC and JB-HUVEC group were analyzed. Western blot experiments showed that the Akt protein content in HUVECs stimulated with JB (40  $\mu\text{g}/\text{ml}$ , 60  $\mu\text{g}/\text{ml}$ , and 80  $\mu\text{g}/\text{ml}$ ) decreased by 21.4%, 11.1%, and 15.9%, respectively, compared with the Akt protein content of HUVECs stimulated with JA for the same concentrations (Figure 8A, 8B). The STAT3 protein content in the JB-HUVEC groups was only 79.3%, 69.3%, and 54.7% of the corresponding concentrations in the JA-HUVEC groups (Figure 8A, 8C). Additionally, the mTOR protein content in the JB-HUVEC groups was only 25.7%, 11.6%, and 34.1% of the corresponding concentrations in JA-HUVEC groups, respectively (Figure 8A, 8D). These results indicate that, with increasing concentrations of JA or JB, the expressions of Akt, STAT3, and mTOR proteins in

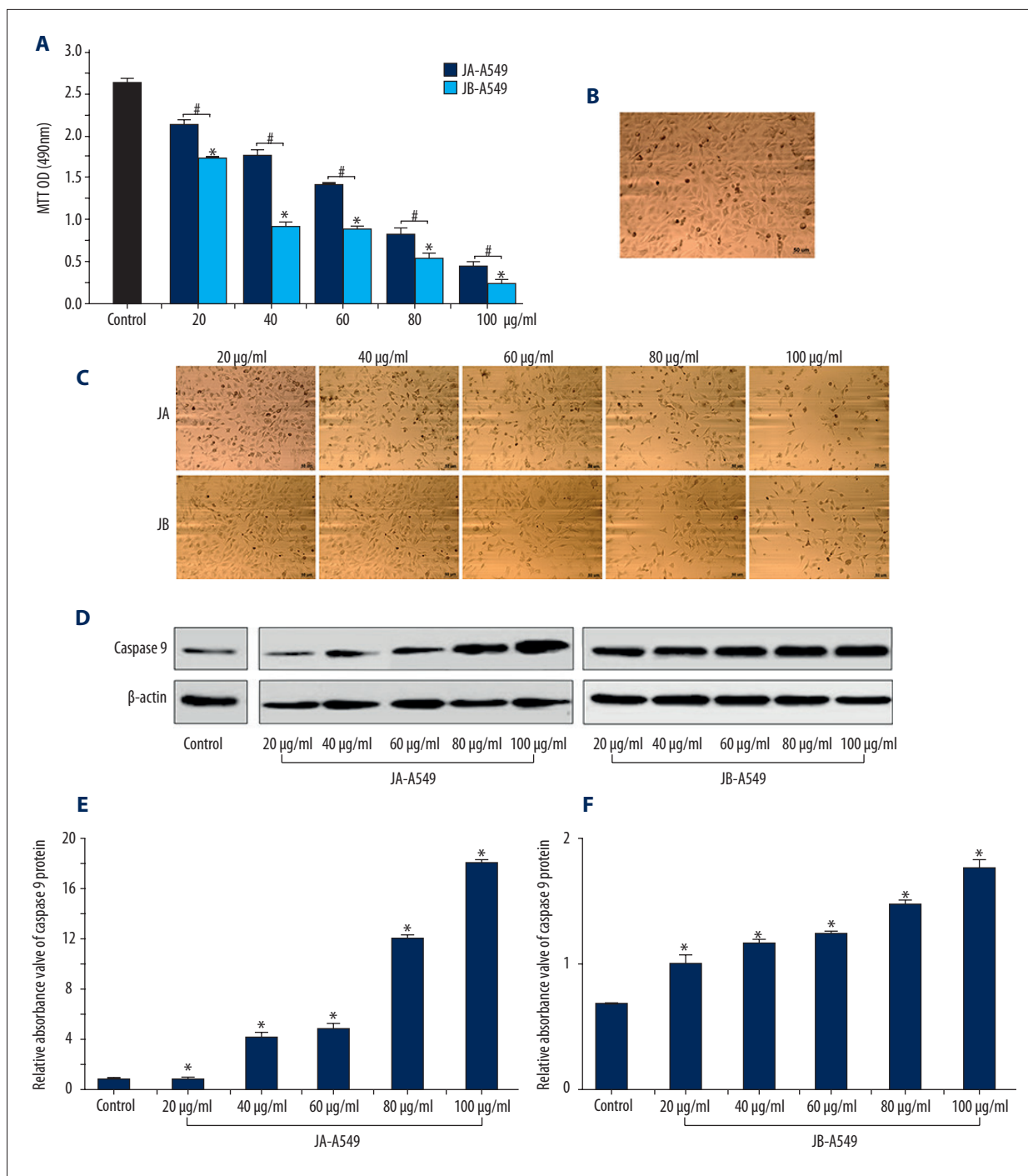


**Figure 2.** JA and JB separately inhibited A549 cell proliferation and promoted apoptosis. **(A)** An MTT assay with OD values (490 nm) for A549 cells from each group, cultured for 24 h. \*  $P < 0.01$ , compared with the control group. #  $P < 0.01$  indicates a significant difference between JA and JB at the same concentration. Each value represents the mean  $\pm$ SE of triplicate tests. **(B)** Photograph of the normal cultured A549 cells after 24 h (scale bar=50µm). **(C)** Photographs of the A549 cells stimulated by JA or JB of 20 µg/ml, 40 µg/ml, 60 µg/ml, 80 µg/ml, and 100 µg/ml concentrations after 24 h. (Scale bar=50µm). **(D)** The Western blot images of JA and JB promotion of caspase 9 protein expression in A549 cells. **(E F)** The relative absorbance values of caspase 9 protein bands. JA-A549 groups **(E)**, JB-A549 groups **(F)**. All \*  $P < 0.01$ . Each value represents the mean  $\pm$ SE of triplicate tests.

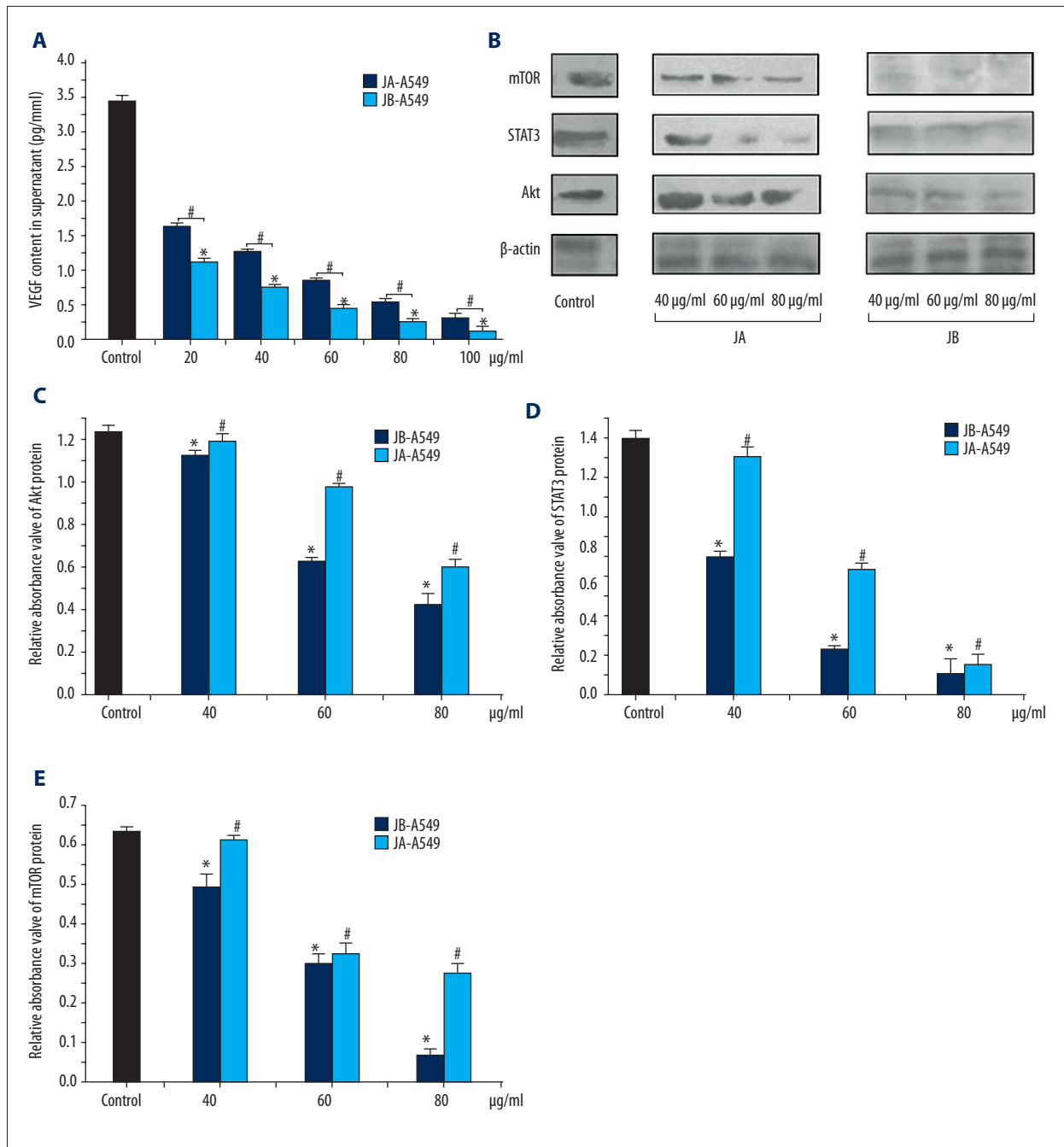


**Figure 3.** JA and JB each affected the expression of the VEGF protein in A549 cells by inhibiting the Akt-STAT3-mTOR signaling pathway. **(A)** The VEGF content in the supernatant of each group, \*  $P < 0.01$ , compared with the control group. #  $P < 0.01$  indicates a significant difference between JA and JB at the same concentration. Each value represents the mean  $\pm$ SE of triplicate tests. **(B)** The Western blot images showing the effects of JA and JB on the expression of mTOR, STAT3, and Akt proteins in A549 cells. **(C–E)** The relative absorbance values of Akt, STAT3, and mTOR protein bands in the control, JA-A549, and JB-A549 groups. The relative absorbance values of the Akt protein **(C)**, the relative absorbance values of the STAT3 protein **(D)**, the relative absorbance values of the mTOR protein **(E)**. All \*  $P < 0.01$ , JB-A549 groups, All #  $P < 0.01$ , JA-A549 groups. Each value represents the mean  $\pm$ SE of triplicate tests.

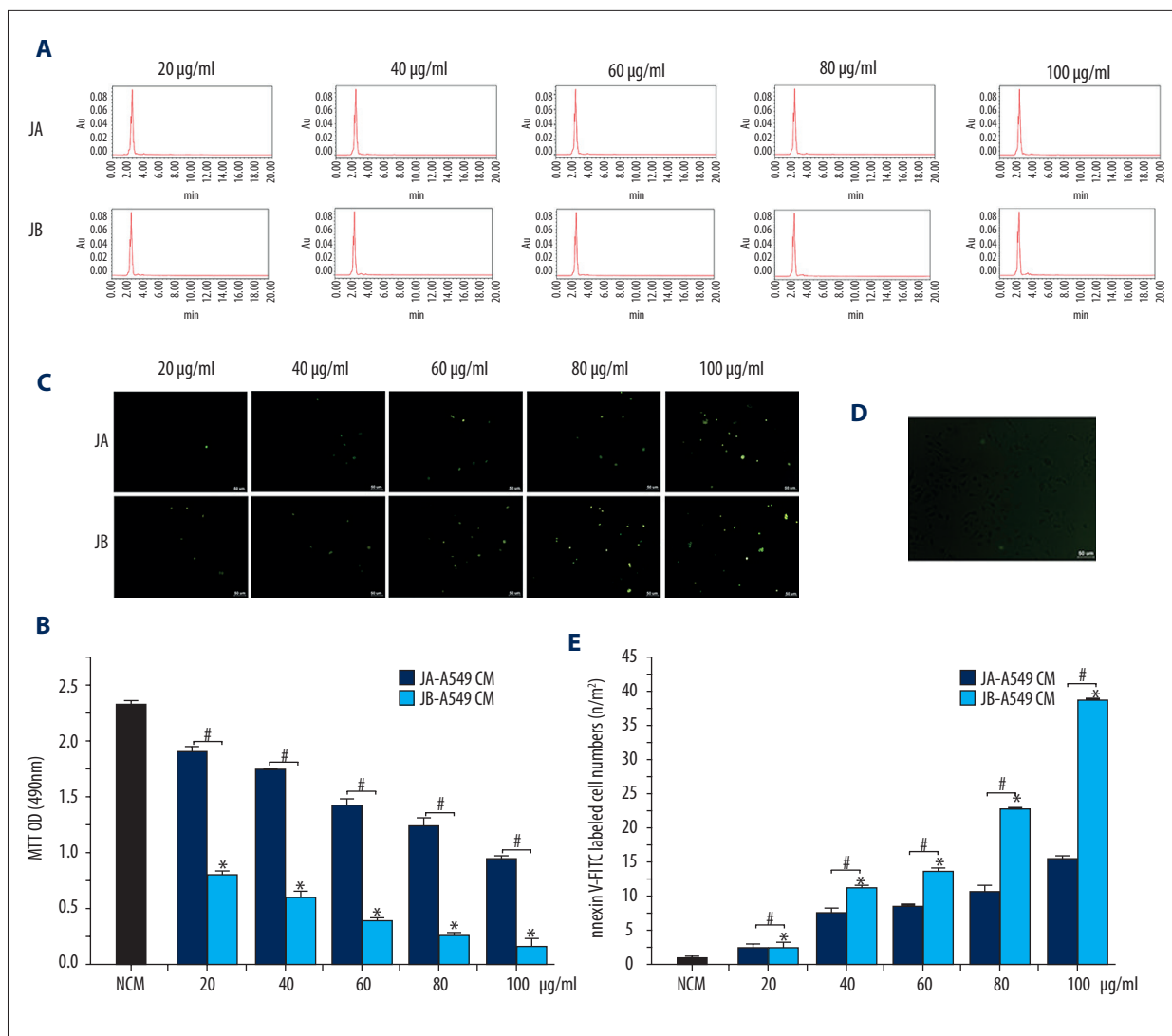


**Figure 4.** The conditioned media (CM) of A549 cells stimulated by JA or JB were both shown to inhibit HUVEC proliferation and promoted HUVEC apoptosis. **(A)** The detection of residual JA or JB in each CM (JA-A549 CM and JB-A549 CM groups) by liquid chromatography. **(B)** An MTT assay with the OD values (490 nm) for HUVECs from each group, cultured for 24 h. \*  $P < 0.01$ , compared with the control group. #  $P < 0.01$  indicates a significant difference between JA and JB at the same concentration. Each value represents the mean  $\pm$ SE of triplicate tests. **(C, D)** Photographs of Annexin V-FITC labeled HUVEC apoptosis. JA-A549 CM and JB-A549 CM **(C)**, NCM group **(D)** (scale bar=50  $\mu$ m). **(E)** The Annexin V-FITC labeled HUVEC numbers for each group. \*  $P < 0.01$ , compared with the control group. #  $P < 0.01$  indicates a significant difference between JA and JB at the same concentration. Each value represents the mean  $\pm$ SE of triplicate tests.

HUVECs gradually decreased, which may be due to the direct inhibition of the relevant signaling pathways.

### Jolkinolides reduced the expression of the VEGF protein in A549 cell xenograft tumors

We inoculated A549 cells into nude mice to create xenograft tumor models. Immunohistochemical staining of the VEGF protein was performed, demonstrating that, with increasing concentrations of JB, the expression of VEGF gradually decreased on

the 30<sup>th</sup>, 45<sup>th</sup>, and 60<sup>th</sup> day after the administration (Figure 9). This suggests that JB is capable of directly reducing VEGF protein expression in xenografted tumor tissue.

### Discussion

Lung, breast, and other malignant cancers are increasingly important threats to human health [1–3]. In recent years, the number of deaths due to breast and lung cancers has been



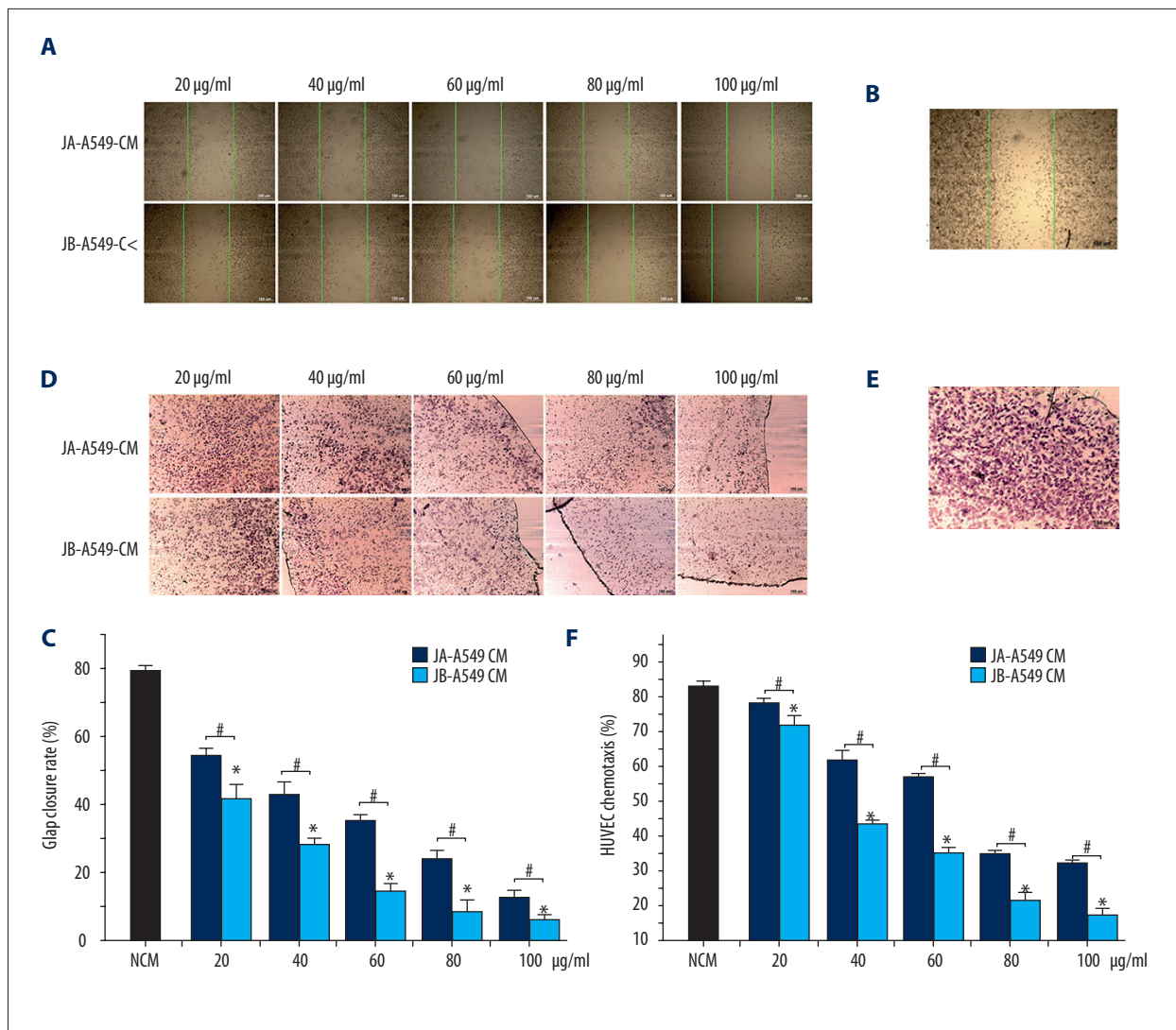


**Figure 5.** The conditioned media (CM) from A549 cells stimulated by JA and JB separately inhibited HUVEC migration. (A, B) Photographs of scratches in HUVECs cultured for 24 h. The green lines represent the cell scratch area at 0 h. JA-A549 CM and JB-A549 CM (A), NCM group (B) (scale bar=150 µm). (C) The scratch closure rate in HUVECs cultured for 24 h. \*  $P < 0.01$ , compared with the control group. #  $P < 0.01$  indicates a significant difference between JA and JB at the same concentration. Each value represents the mean  $\pm$ SE of triplicate tests. (D, E) Migration of HUVECs. JA-A549 CM and JB-A549 CM groups (D), NCM group (E) (scale bar=150 µm). (F) The effect of the conditioned medium on HUVEC migration. \*  $P < 0.01$ , compared with the control group. #  $P < 0.01$  indicates a significant difference between JA and JB at the same concentration. Each value represents the mean  $\pm$ SE of triplicate tests.

on a steady increase, a problem that has serious ramifications on social and economic development [1–3]. Therefore, the effective inhibition of the growth and metastasis of tumors is critically important for improving the prognosis and quality of life of cancer patients.

It has been reported that, for tumors greater than 2 mm in diameter, the tumor tissues need significantly greater levels of oxygen and nutrition supplied by the local blood vessels [23,24]. As a result, a degradation or atrophy of tumor tissues

occurs if the capillaries and small vessels in tumor tissues are inadequate. Peripheral blood vessels in tumor tissues provide a suitable environment for the proliferation and detachment of tumor cells, which explains why tumor vessels are closely associated with tumor growth and metastasis [23,25]. Currently, surgical excision, chemotherapy, radiotherapy, and immunotherapy are still the most effective approaches for the treatment of many cancers. However, chemotherapy and radiotherapy usually lead to serious adverse effects, such as impairment of the hematopoietic and immune systems [26]. With

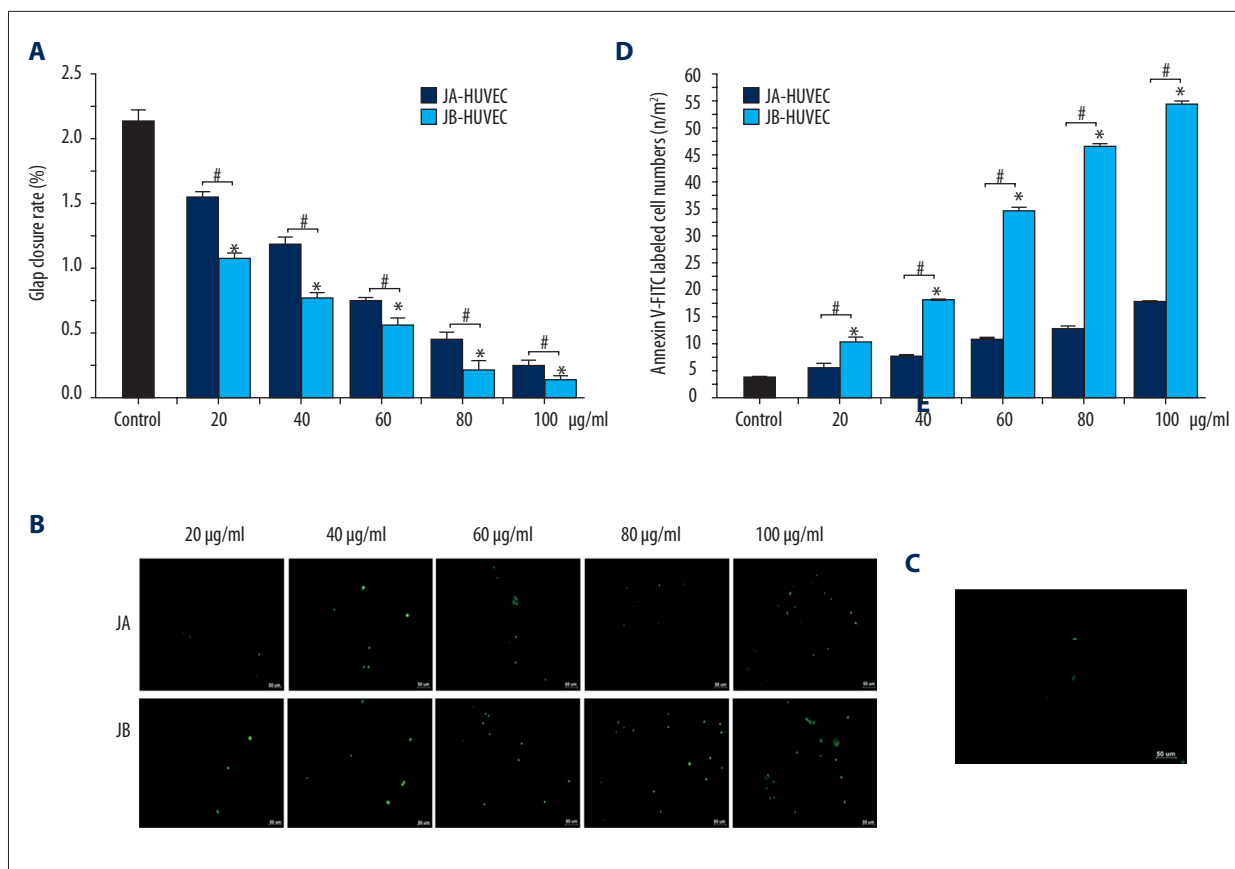


**Figure 6.** JA and JB inhibited HUVEC proliferation and promoted HUVEC apoptosis. **(A)** An MTT assay with the OD values (490 nm) for HUVECs from each group cultured for 24 h. \*  $P < 0.01$ , compared with the control group. #  $P < 0.01$  indicates a significant difference between JA and JB at the same concentration. Each value represents the mean  $\pm$ SE of triplicate tests. **(B, C)** Photographs of Annexin V-FITC labeled HUVEC apoptosis. JA-HUVEC groups and JB-HUVEC groups **(B)**, the control group **(C)** (scale bar=50  $\mu$ m). **(D)** The Annexin V-FITC labeled HUVEC numbers for each group. \*  $P < 0.01$ , comparison of the control group. #  $P < 0.01$  indicates a significant difference between JA and JB at the same concentration. Each value represents the mean  $\pm$ SE of triplicate tests.

the rapid development of traditional Chinese medicine with modern medical technologies in the last several decades, numerous studies have found that *E. fischeriana* Steud [27,28], norcantharidin [29], lycorine [30], curcumin [31], and other plant products have significant anti-tumor activities, including the inhibition of tumor cell growth and metastasis. In addition, most traditional Chinese medicines have significantly fewer adverse effects than chemotherapy, but with comparable therapeutic effects [32]. Identification of natural plant ingredients with growth inhibition and anti-angiogenic properties is of great significance for the treatment of cancer.

*E. fischeriana* Steud, *Euphorbia ebracteolata* Hayata, and over 2000 other species of the *Euphorbia* genus are found in Europe, Asia, and other continents [33,34]. A number of studies have reported on the broad-spectrum anti-tumor activity of *E. fischeriana* [35], which has also been shown to exhibit anti-HIV and anti-epileptic activities [36] and has been used for the treatment

of edema, ascites, and pleural effusion [10,11,37]. Compounds extracted from plants typically have fewer adverse effects compared with man-made drugs. Therefore, natural plant drugs have attracted increasing attention in biomedical research.

Studies found that *E. fischeriana* Steud contains abundant compounds, including diterpenoids, flavonoids, coumarins, and more than 60 other compounds [15]. The diterpenoids in the root of *E. fischeriana* Steud include Jolkinolide A (JA), Jolkinolide B (JB), 17-hydroxy-jolkinolide B, 17-hydroxy-jolkinolide A, 12-Deoxyphorbol 13-palmitate, and many other compounds [38]. 17-Hydroxy-jolkinolide A inhibits osteoclast differentiation through suppressing the activation of NF- $\kappa$ B and MAPKs [39]. Studies have also found that Pekinenin C and others extracts from this plant can decrease swelling, reduce tissue fluid exudation, and reduce the exudation of pleural effusion or ascites [40]. 12-Deoxyphorbol 13-palmitate has also been shown to inhibit tumor angiogenesis [19]. These suggest

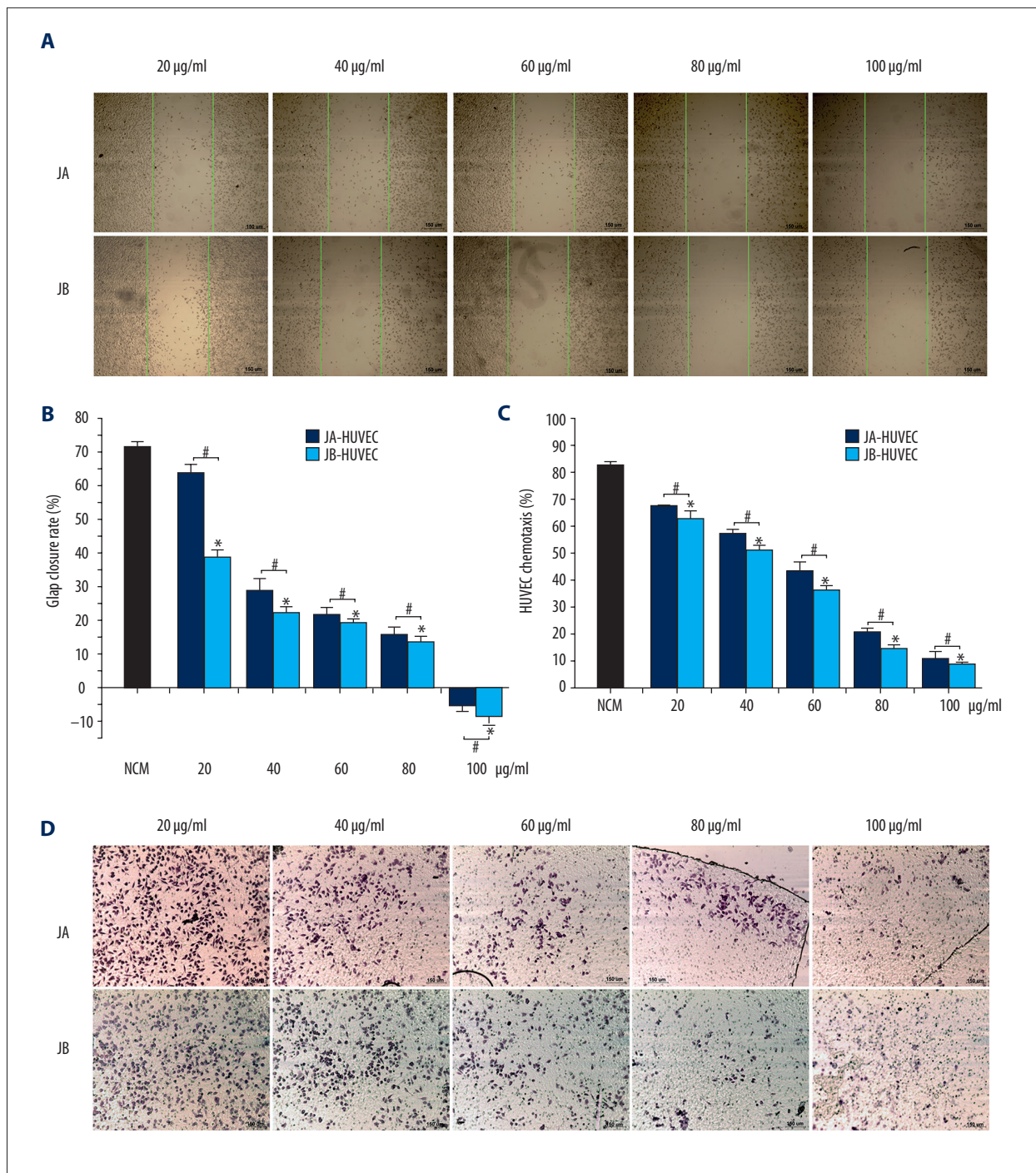


**Figure 7.** JA and JB inhibited HUVEC migration. **(A)** Scratch photos for HUVECs from each group, cultured for 24 h. The green lines represent the cell scratch area at 0 h (scale bar=150µm). **(B)** The scratch closure rate in HUVECs cultured for 24 h. \*  $P<0.01$ , compared with the control group. #  $P<0.01$  indicates a significant difference between JA and JB at the same concentration. Each value represents the mean  $\pm$ SE of triplicate tests. **(C)** The effects of JA (or JB) on HUVEC migration. \*  $P<0.01$ , compared with the control group. #  $P<0.01$  indicates a significant difference between JA and JB at the same concentration. Each value represents the mean  $\pm$ SE of triplicate tests. **(D)** Migration of the HUVECs from JA-HUVEC groups and JB-HUVEC groups (scale bar=150 µm).

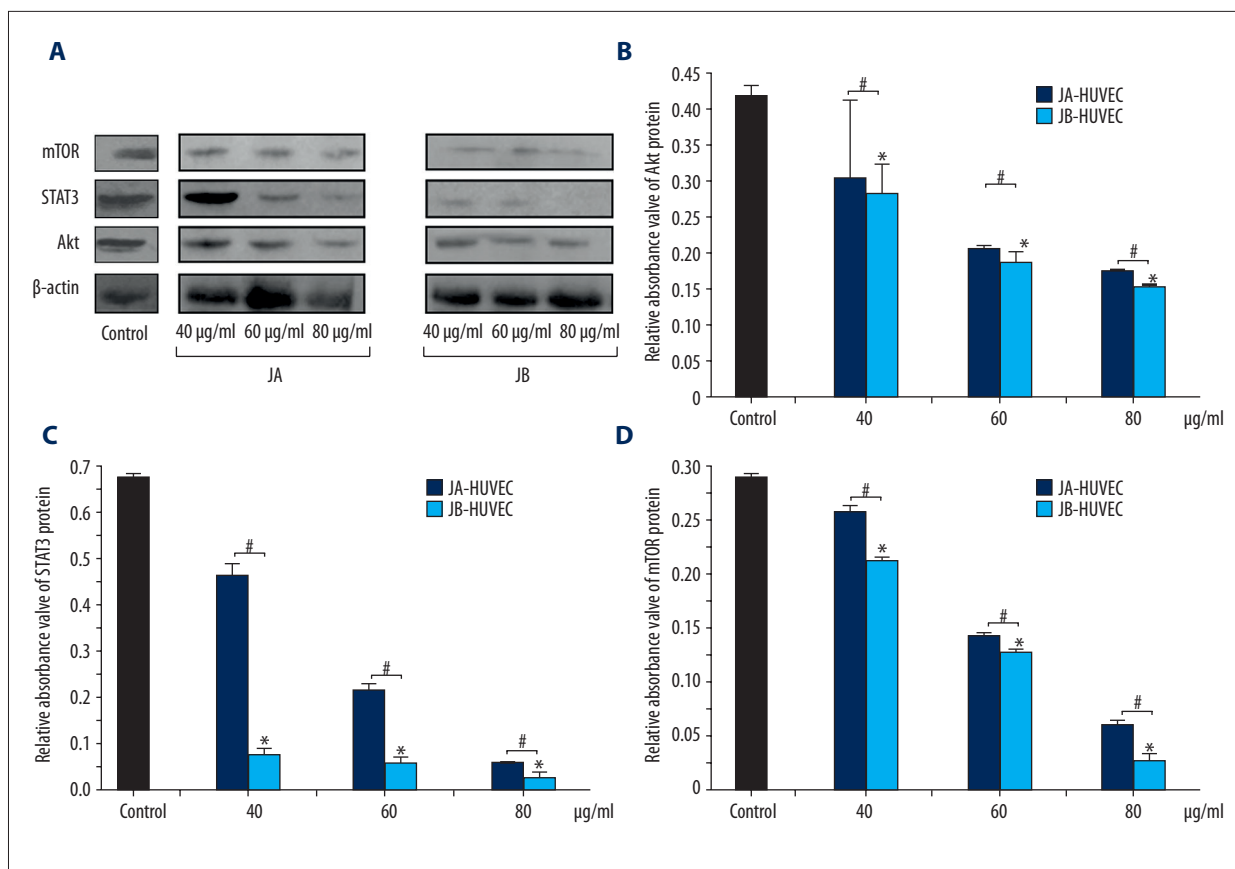


**Figure 8.** JA and JB separately inhibited the expression of Akt, STAT3, and mTOR proteins in HUVECs. (A) The Western blot images of the effects of JA and JB on the expression of mTOR, STAT3, and Akt proteins. (B–D) The relative absorbance values of Akt, STAT3, and mTOR protein bands in the control group, JA-HUVEC groups and JB-HUVEC groups. The relative absorbance values of Akt protein (B), the relative absorbance values of STAT3 protein (C), the relative absorbance values of mTOR protein (D). All \*  $P < 0.01$ , compared with the control group. #  $P < 0.01$  indicates a significant difference between JA and JB at the same concentration. Each value represents the mean  $\pm$ SE of triplicate tests.

that the diterpenoids in the root of *E. fischeriana* Steud may have anti-angiogenic properties or may alter vascular permeability. Therefore, basic research on the effective components and pharmacodynamic properties of *E. fischeriana* Steud, particularly on its anti-angiogenic activities, would be helpful in the selection of potential therapies.

In this study, we analyzed the effects of JA and JB on A549 cells. The MTT assay showed that the inhibitory effects of JB were more obvious in A549 cells than were those of JA (Figure 2A–2C). With increasing JB concentrations, the OD values of A549 cell proliferation gradually decreased, and caspase 9 protein expression was shown to significantly increase in all JB-treated A549 cells (Figure 2D–2F). This demonstrates that Jolkinolides activity inhibits A549 cells in a dose-dependent manner (Figure 2). In agreement with our results, Kuang found that the diterpenoids in the roots of *E. fischeriana* Steud significantly inhibited the growth of MCF-7 cells and increased the apoptosis rate of tumor cells [27]. This means

that the studied diterpenoids have anti-tumor activity. Other studies have found that JB stimulated the down-regulation of JAK2/STAT3 protein expression in human leukemia cells and stimulated the up-regulation of intracellular BCL-2, Bax, and cytochrome C expression. In addition, JB was also shown to trigger the activity of caspase-3, caspase-8, and caspase-9 to induce apoptosis [41]. STAT3 and mTOR proteins are important in the Akt signaling pathway, which plays a key role in cell growth and movement [42]. Some studies have also found that 17-Hydroxy-JB strongly inhibited the STAT3 protein and disrupted cell metabolism and growth, thus promoting the apoptosis of HepG2 and other tumor cells [43]. We therefore intend to further explore whether JA and JB affect the activity of tumor cell proliferation and apoptosis through the Akt-STAT3-mTOR signaling pathway.

The expression of Akt-STAT3-mTOR proteins in A549 cells gradually decreased upon exposure to either JA or JB (Figure 3B–3E), and VEGF and other cytokines secreted by A549 cells were

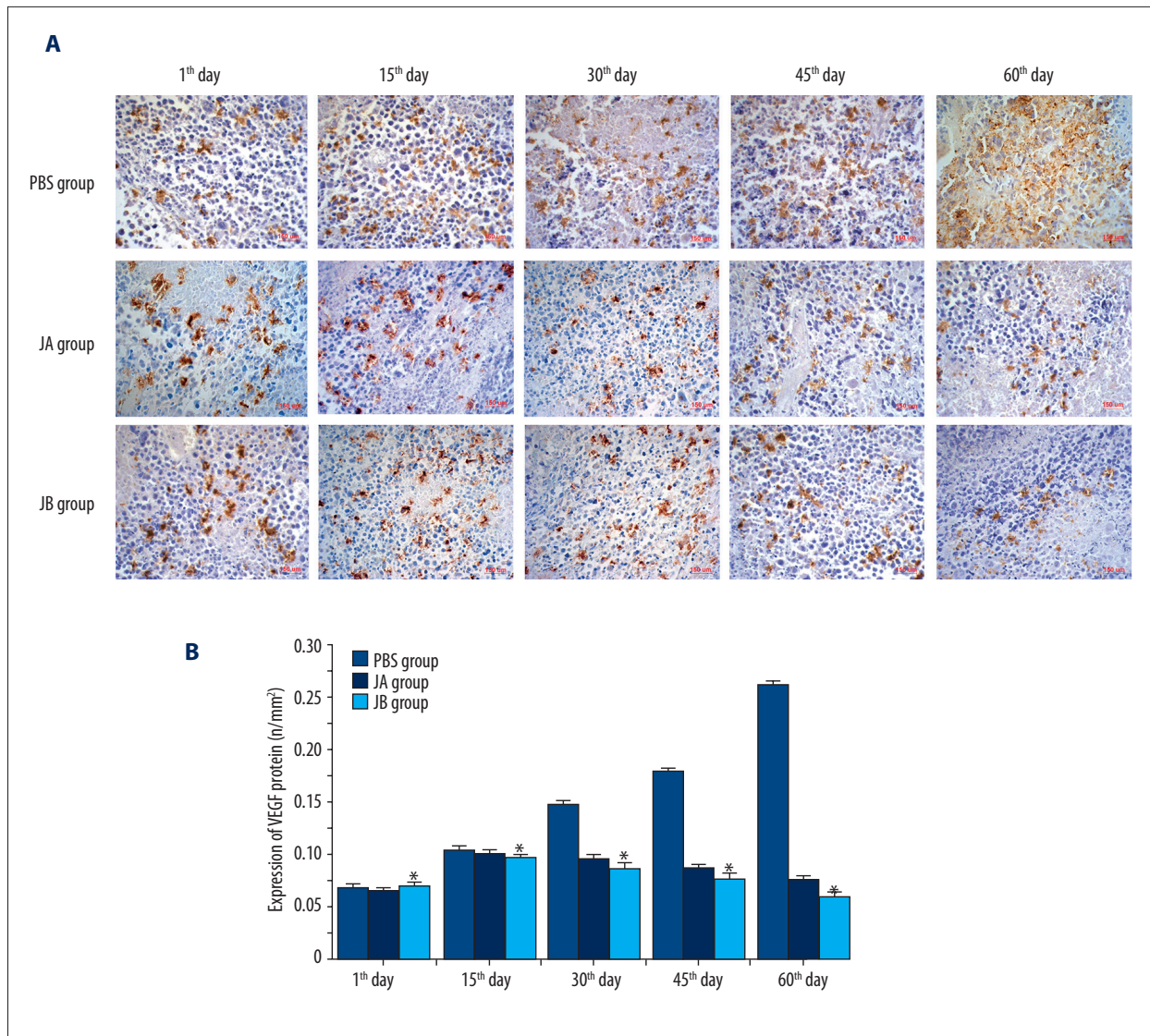


**Figure 9.** JA and JB inhibited the expression of the VEGF protein in A549 cell xenograft tumor. **(A)** Photomicrographs showing immunohistochemical staining for the expression of the VEGF protein in the A549 cell xenograft tumor of each group (scale bar=150  $\mu$ m). **(B)** The expression of VEGF protein on the first, 10<sup>th</sup>, 30<sup>th</sup>, 45<sup>th</sup>, and 60<sup>th</sup> day of administration for each group. \*  $P < 0.01$ , comparison with the control group. Each value represents the mean  $\pm$  SE of triplicate tests.

shown to decrease as well (Figure 3A). These results may be due to the inhibition of VEGF gene transcription through the inhibition of Akt or STAT3 proteins in the Akt signaling pathway [44,45]. It is interesting that 12-Deoxy-phorbol-13-palmitate has also been demonstrated to inhibit the Akt/mTOR signaling pathway and to reduce VEGF or HIF-1 $\alpha$  expression in MCF-7 cells [20]. These findings are similar to the results of our study.

In the human body, tumor tissues secrete a large amount of CXCL-8 and other cytokines, thereby promoting angiogenesis [46]. The creation of new vascular tissue allows for increased nutritional availability and facilitates the rapid growth and metastasis of the tumor. Therefore, tumor tissues and the

peripheral blood vessels have been shown to interact with each other [23,25]. To clarify the relationship between tumor cells and HUVECs, we first removed the supernatant from JA and JB by centrifugation and used liquid chromatography to prove that there was no residual JA or JB in any of the supernatant samples (Figure 4A). This method ensured that there would be no interference from JA or JB on the HUVECs cultured in the conditioned media. The A549-conditioned media was used to culture the HUVECs. We found that both the JA-A549-CM and JB-A549-CM groups reduced the OD values of HUVEC proliferation (Figure 4B) and enhanced HUVEC apoptosis (Figure 4C–4E). We then found that the conditioned media also inhibited the HUVEC scratch closure and migration rates

(Figure 5). However, the inhibitory effect on HUVEC movement was more obvious in JB (Figure 5C, 5F). These results demonstrate that both conditioned media were capable of inhibiting HUVEC migration. The Western blot results showed that the Akt-STAT3-mTOR proteins in A549 cells gradually decreased with increasing concentrations of JA or JB (Figure 3B–3E), further demonstrating that Jolkinolides reduce the secretion of active vascular endothelial cells factors in tumor cells through the inhibition of the Akt signaling pathway.

We then used JA and JB in varying concentrations to stimulate HUVECs and found that the OD values of HUVEC proliferation in the JB-HUVEC groups were significantly lower than those in the JA-HUVEC groups (Figure 6A), and that the Jolkinolides inhibition of HUVEC proliferation and migration operates in a dose-dependent manner. These results suggest that both JA and JB inhibit HUVEC proliferation, promote HUVEC apoptosis, and decrease HUVEC migration through inhibition of the Akt signaling pathway (Figures 7, 8). Therefore, JB has significant and important inhibitory effects on HUVEC growth.

VEGF is key for the formation and growth of tumor blood vessels and is integral to the invasion and metastasis of breast cancer, as well as other malignant tumors [47]. Anti-angiogenesis has become a research highlight in the study of traditional Chinese medicines. Our experiments found that JB has inhibitory effects on the expression of VEGF in A549 xenograft tumors (Figure 9) and on HUVEC migration (Figure 7), thus showing similar activities as 12-Deoxyphorbol 13-palmitate, another diterpenoid found in *E. fischeriana* Steud [19]. These effects are summarized in the ability of Jolkinolides to decrease HUVEC activity and angiogenesis through the inhibition of the Akt/mTOR signaling pathway in A549 cells and HUVECs. The Akt signaling pathway plays a very important role in the process of vascular formation (Figures 3, 8) [48,49]; the activation of the Akt signaling pathway promotes the contraction of cell microfilaments and microtubules and the formation of a pseudopod, ultimately encouraging cell movement and migration [50]. In the process of angiogenesis, the movement and migration of HUVECs are closely related to the intracellular Akt signaling pathway [51]. The continuous endogenous activation of this pathway can induce the abnormal proliferation seen in tumor tissues by influencing both morphology and function. STAT3/mTOR is a kind

of serine/threonine protein kinase, and is an important downstream molecule in the Akt signaling pathway. The STAT3/mTOR protein is critical during tumor initiation and malignancy progression and is an important target for cancer treatment [52]. During the abnormal proliferation of tumor tissue, the tumor cells activate the Akt/STAT3/mTOR proteins to induce the expression of HIF-1 $\alpha$  or VEGF, which are downstream targets of the Akt signaling pathway, thereby accelerating angiogenesis [53]. According to our experimental results and the literature analyses, we believe that the diterpenoids found in *E. fischeriana* Steud will become new targets for the development of novel, natural anti-angiogenic therapies.

In conclusion, JA and JB induced apoptosis in A549 cells and HUVECs. They were also shown to inhibit A549 paracrine vascular endothelial cell factors through the inhibition of the Akt/STAT3/mTOR signaling pathway, thereby playing an inhibitory role in HUVECs *in vitro*. Nevertheless, we cannot exclude the possibility that these Jolkinolides may also act similarly to other diterpenoids in the inhibition of the MAPK, ERK, or other signaling pathways [10,54]. Therefore, further studies are necessary to discern the mechanism underlying the action of these signaling pathways and to determine their potential application in treating human cancers. In future research, we will focus on the use of animal models of human cancer to confirm the effects of JA and JB on tumor angiogenesis *in vivo*, and to lay a foundation for the extensive use of *E. fischeriana* Steud and other plants for the inhibition of tumor growth and angiogenesis.

## Conclusions

JB not only inhibits the secretion of vasoactive cytokines in A549 cells, but also directly inhibits HUVEC activity through influencing the Akt/STAT3/mTOR signaling pathway, achieving an inhibitory effect on HUVECs and preventing tumor angiogenesis. These preclinical findings offer new perspectives for the use of *E. fischeriana* Steud and other natural plants in the treatment of human cancer.

## Conflict of interests

The authors declare that there is no conflict of interests.

## References:

- Chen W, Zheng R, Baade PD et al: Cancer statistics in China, 2015. *Cancer J Clin*, 2016; 66: 115–32
- Smith RA, Andrews K, Brooks D et al: Cancer screening in the United States, 2016: A review of current American Cancer Society guidelines and current issues in cancer screening. *Cancer J Clin*, 2016; 66: 96–114
- Torre LA, Bray F, Siegel RL et al: Global cancer statistics, 2012. *Cancer J Clin*, 2015; 65: 87–108
- Senkus E, Kyriakides S, Ohno S et al: Primary breast cancer: ESMO Clinical Practice Guidelines for diagnosis, treatment and follow-up. *Ann Oncol*, 2015; 26(Suppl. 5): v8–30
- Casey SC, Amedei A, Aquilano K et al: Cancer prevention and therapy through the modulation of the tumor microenvironment. *Semin Cancer Biol*, 2015; 35(Suppl): S199–223
- Shen J, Kai J, Tang Y et al: The chemical and biological properties of *Euphorbia kansui*. *Am J Chin Med*, 2016; 44: 253–73

7. Wang M, Wang Q, Wei Q et al: Two new ent-atisanes from the root of *Euphorbia fischeriana* Steud. *Nat Prod Res*, 2016; 30: 144–49
8. Han MH, Lee WS, Nagappan A et al: Polyphenols from Korean prostrate spurge *Euphorbia supina* induce apoptosis through the Fas-associated extrinsic pathway and activation of ERK in human leukemic U937 cells. *Oncol Rep*, 2016; 36: 99–107
9. Liu J, Sun Y, Liu L, Yu C: A water-soluble polysaccharide (EFP-AW1) from the alkaline extract of the roots of a traditional Chinese medicine, *Euphorbia fischeriana*: Fraction and characterization. *Carbohydr Polym*, 2012; 88: 1299–303
10. Uto T, Qin GW, Morinaga O, Shoyama Y: 17-Hydroxy-jolkinolide B, a diterpenoid from *Euphorbia fischeriana*, inhibits inflammatory mediators but activates heme oxygenase-1 expression in lipopolysaccharide-stimulated murine macrophages. *Int Immunopharmacol*, 2012; 12: 101–9
11. Sun YX, Liu JC: Chemical constituents and biological activities of *Euphorbia fischeriana* Steud. *Chem Biodivers*, 2011; 8: 1205–14
12. Pan LC, Xu XH, Zhang NN et al: HJB-1, a 17-hydroxy-jolkinolide B derivative, inhibits LPS-induced inflammation in mouse peritoneal macrophages. *Int Immunopharmacol*, 2014; 21: 474–80
13. Yang H, Li Y, Huo P et al: Protective effect of Jolkinolide B on LPS-induced mouse acute lung injury. *Int Immunopharmacol*, 2015; 26: 119–24
14. Nogueira IA, Leão AB, Vieira MS et al: Antitumor and antiangiogenic activity of *Synadenium umbellatum* Pax. *J Ethnopharmacol*, 2008; 120: 474–78
15. Vasas A, Hohmann J: *Euphorbia diterpenes*: Isolation, structure, biological activity, and synthesis (2008–2012). *Chem Rev*, 2014; 114: 8579–612
16. Reis MA, Paterna A, Mónico A et al: Diterpenes from *Euphorbia piscatoria*: Synergistic interaction of Lathyranes with doxorubicin on resistant cancer cells. *Planta Med*, 2014; 80: 1739–45
17. Xu HY, Chen ZW, Li H et al: 12-Deoxyphorbol 13-palmitate mediated cell growth inhibition, G2-M cell cycle arrest and apoptosis in BGC823 cells. *Eur J Pharmacol*, 2013; 700: 13–22
18. Li Y, Liu XL, Cai ZG, Zhang SX: LC-ESI-MS/MS analysis and pharmacokinetics of Jolkinolide B, a potential antitumor active component isolated from *Euphorbia fischeriana*, in rat plasma. *Biomed Chromatogr*, 2014; 28: 193–96
19. Xu HY, Pan YM, Chen ZW et al: 12-Deoxyphorbol 13-palmitate inhibit VEGF-induced angiogenesis via suppression of VEGFR-2-signaling pathway. *J Ethnopharmacol*, 2013; 146: 724–33
20. Yang Y, Cong H, Han C et al: 12-Deoxyphorbol 13-palmitate inhibits the expression of VEGF and HIF-1 $\alpha$  in MCF-7 cells by blocking the PI3K/Akt/mTOR signaling pathway. *Oncol Rep*, 2015; 34: 1755–60
21. Lee JW, Lee C, Jin Q et al: Diterpenoids from the roots of *Euphorbia fischeriana* with inhibitory effects on nitric oxide production. *J Nat Prod*, 2016; 79: 126–31
22. Shen L, Wang P, Yang J, Li X: MicroRNA-217 regulates WASF3 expression and suppresses tumor growth and metastasis in osteosarcoma. *PLoS One*, 2014; 9: e109138
23. Bhat TA, Singh RP: Tumor angiogenesis – a potential target in cancer chemoprevention. *Food Chem Toxicol*, 2008; 46: 1334–45
24. Blonska M, Agarwal NK, Vega F: Shaping of the tumor microenvironment: Stromal cells and vessels. *Semin Cancer Biol*, 2015; 34: 3–13
25. Nambiar DK, Kujur PK, Singh RP: Angiogenesis assays. *Methods Mol Biol*, 2016; 1379: 107–15
26. van Vuuren RJ, Visagie MH, Theron AE, Joubert AM: Antimitotic drugs in the treatment of cancer. *Cancer Chemother Pharmacol*, 2015; 76: 1101–12
27. Kuang X, Li W, Kanno Y et al: ent-Atisanes diterpenoids from *Euphorbia fischeriana* inhibit mammosphere formation in MCF-7 cells. *J Nat Med*, 2016; 70: 120–26
28. Shadi S, Saedi H, Ghanadian M et al: New macrocyclic diterpenes from *Euphorbia connata* Boiss. with cytotoxic activities on human breast cancer cell lines. *Nat Prod Res*, 2015; 29: 607–14
29. Peng C, Li Z, Niu Z et al: Norcantharidin suppresses colon cancer cell epithelial-mesenchymal transition by inhibiting the  $\alpha$ v $\beta$ 6-ERK-Ets1 signaling pathway. *Sci Rep*, 2016; 6: 20500
30. Wang P, Yuan HH, Zhang X et al: Novel lycorine derivatives as anticancer agents: Synthesis and *in vitro* biological evaluation. *Molecules*, 2014; 19: 2469–80
31. Fan H, Liang Y, Jiang B et al: Curcumin inhibits intracellular fatty acid synthase and induces apoptosis in human breast cancer MDA-MB-231 cells. *Oncol Rep*, 2016; 35: 2651–56
32. Ji Q, Luo YQ, Wang WH et al: Research advances in traditional Chinese medicine syndromes in cancer patients. *J Integr Med*, 2016; 14: 12–21
33. Horn JW, van Ee BW, Morawetz JJ et al: Phylogenetics and the evolution of major structural characters in the giant genus *Euphorbia* L. (Euphorbiaceae). *Mol Phylogenet Evol*, 2012; 63: 305–26
34. Ernst M, Sasilis-Lagoudakis CH, Grace OM et al: Evolutionary prediction of medicinal properties in the genus *Euphorbia* L. *Sci Rep*, 2016; 6: 30531
35. Yang DS, Peng WB, Yang YP et al: Chemical constituents from *Euphorbia wallichii* and their biological activities. *J Asian Nat Prod Res*, 2015; 17: 946–51
36. Jiang C, Luo P, Zhao Y et al: Carolignans from the aerial parts of *Euphorbia sikkimensis* and their anti-HIV activity. *J Nat Prod*, 2016; 79: 578–83
37. Majid M, Khan MR, Shah NA et al: Studies on phytochemical, antioxidant, anti-inflammatory and analgesic activities of *Euphorbia dracunculoides*. *BMC Complement Altern Med*, 2015; 15: 349
38. King AJ, Brown GD, Gilday AD et al: Production of bioactive diterpenoids in the euphorbiaceae depends on evolutionarily conserved gene clusters. *Plant Cell*, 2014; 26: 3286–98
39. Wang Y, Xu X, Wang HB et al: 17-Hydroxy-jolkinolide A inhibits osteoclast differentiation through suppressing the activation of NF- $\kappa$ B and MAPKs. *Int Immunopharmacol*, 2015; 29: 513–20
40. Cao Y, Cheng F, Yao W et al: Toxicity of Pekinenin C from *Euphorbia pekinensis* radix on rat small intestinal crypt epithelial cell and its apoptotic mechanism. *Int J Mol Sci*, 2016; 17: E850
41. Wang JH, Zhang K, Niu HY et al: Jolkinolide B from *Euphorbia fischeriana* Steud induces in human leukemic cells apoptosis via JAK2/STAT3 pathways. *Int J Clin Pharmacol Ther*, 2013; 51: 170–78
42. Chen YC, Chien LH, Huang BM et al: Aqueous extracts of *Toona sinensis* leaves inhibit renal carcinoma cell growth and migration through JAK2/stat3, Akt, MEK/ERK, and mTOR/HIF-2 $\alpha$  pathways. *Nutr Cancer*, 2016; 68: 654–66
43. Wang Y, Ma X, Yan S et al: 17-hydroxy-jolkinolide B inhibits signal transducers and activators of transcription 3 signaling by covalently cross-linking Janus kinases and induces apoptosis of human cancer cells. *Cancer Res*, 2009; 69: 7302–10
44. Liu Y, Luo F, Wang B et al: STAT3-regulated exosomal miR-21 promotes angiogenesis and is involved in neoplastic processes of transformed human bronchial epithelial cells. *Cancer Lett*, 2016; 370: 125–35
45. Wang H, Zhang C, Ning Z et al: Bufalin enhances anti-angiogenic effect of sorafenib via AKT/VEGF signaling. *Int J Oncol*, 2016; 48: 1229–41
46. Liu LB, Xie F, Chang KK et al: Hypoxia promotes the proliferation of cervical carcinoma cells through stimulating the secretion of IL-8. *Int J Clin Exp Pathol*, 2014; 7: 575–83
47. Chamorro-Jorganes A, Lee MY, Araldi E et al: VEGF-induced expression of miR-17-92 cluster in endothelial cells is mediated by ERK/ELK1 activation and regulates angiogenesis. *Circ Res*, 2016; 118: 38–47
48. Wang Y, Nakayama M, Pitulescu ME et al: Ephrin-B2 controls VEGF-induced angiogenesis and lymphangiogenesis. *Nature*, 2010; 465: 483–86
49. Suhasini AN, Wang L, Holder KN et al: A phosphodiesterase 4B-dependent interplay between tumor cells and the microenvironment regulates angiogenesis in B-cell lymphoma. *Leukemia*, 2016; 30: 617–26
50. Bi LK, Zhou N, Liu C et al: Kidney cancer cells secrete IL-8 to activate Akt and promote migration of mesenchymal stem cells. *Urol Oncol*, 2014; 32: 607–12
51. Park H, Lee S, Shrestha P et al: AMIGO2, a novel membrane anchor of PDK1, controls cell survival and angiogenesis via Akt activation. *J Cell Biol*, 2015; 211: 619–37
52. Siveen KS, Sikka S, Surana R et al: Targeting the STAT3 signaling pathway in cancer: Role of synthetic and natural inhibitors. *Biochim Biophys Acta*, 2014; 1845: 136–54
53. Lee YH, Bae HC, Noh KH et al: Gain of HIF-1 $\alpha$  under normoxia in cancer mediates immune adaptation through the AKT/ERK and VEGFA axes. *Clin Cancer Res*, 2015; 21: 1438–46
54. Dong MH, Zhang Q, Wang YY et al: *Euphorbia fischeriana* Steud inhibits malignant melanoma via modulation of the phosphoinositide-3-kinase/Akt signaling pathway. *Exp Ther Med*, 2016; 11: 1475–80